Study On the Effect of Operating Conditions on Acoustic Three-Port Measurements of Perforates in presence of Grazing Flow

Shail A. Shah[1], Hans Bodén[2], and Susann Boij[3]
MWL, Dept. of Engineering Mechanics, KTH Royal Institute of Technology,
Teknikringen 8, SE-100 44 Stockholm

ABSTRACT

Different impedance eduction methods have been previously used to study the acoustic properties of perforated plates in the presence of grazing flow, giving varying results. The work presented here is to contribute to the ongoing experimental research on the acoustic behaviour of perforates under different acoustic excitations and flow conditions. Here, a three-port technique is used to study the aero-acoustic properties of perforates, which allows to observe the acoustic field on both sides of the perforate. Experimentally determined characteristics of the perforate are dependent on the operating conditions like grazing flow speed, microphone distances, standing wave pattern, and temperature. This study aims to provide the experimental analysis on the effect these factors have on the calculated perforate properties, namely the transfer impedance and the scattering matrix.

1. INTRODUCTION

Usage of perforates and micro-perforates for sound attenuation and noise control has gained popularity in the last few decades. Significant research contributing to study the aero-acoustic properties of perforates have been carried out in the last forty years, part of it summarized Refs. [1, 2]. A majority of the research is conducted on aircraft liners, of which perforates are an integral part. Impedance eduction methods are traditionally used to determine the aero-acoustic properties of liners which involve mapping the sound field in the lined section. However, this study involves usage of direct methods for the characterization of the perforates following Ref. [3]. The three-port method for acoustic characterization of perforates is based on Refs. [4, 5], and has been implemented in Refs. [6, 7]. Using the three-port method a study of the aero-acoustic properties of the perforate was made under acoustic excitation from three-directions while under the effect of grazing flow, as shown in Figure 1.

---

[1] shail@kth.se

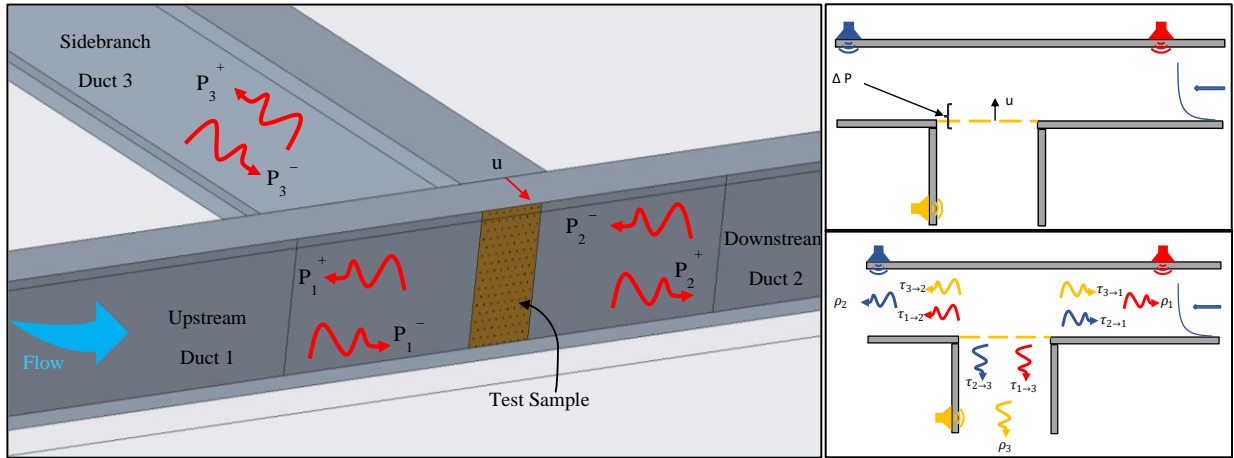[2] hansbod@kth.se

[3] sboij@kth.se

Figure 1 **a.)** Schematic of the three-port setup; **b.)** Calculation of normalized transfer impedance; **c)** Scattering Matrix elements [7]

Key parameters for the characterization of the acoustic properties of a perforate which are of interest in this study are its normalized transfer impedance, and the three-port scattering matrix [4], as shown in Figure 1. Calculation of these properties is carried out in presence of grazing flow using the multi-microphone method, as explained in Ref. [7]. Frequency response functions between the pressure signals acquired by the microphones and a reference signal under stepped sine excitation are considered for calculating the sound field in the three-port. This is done to avoid errors related to the presence of flow noise. Errors related to the acquisition of the pressure signal by the microphones deserve a detailed study of its own, and hence are not covered in the work presented here. However, errors pertaining to the operating conditions during the measurements, e.g., in-duct temperature, microphone positioning and flow velocity affect the calculations significantly and are the focus of this study. Individual effect of these errors on the resulting resistance and S-Matrix coefficients curves is studied and the behaviour of the errors in presence of grazing flow is discussed.

2. ACOUSTIC CHARACTERIZATION

The ratio of difference in the acoustic pressure over the perforate (ΔP) and the particle velocity (u) calculated at the perforate surface is defined as its normalized transfer impedance ($\bar{Z}$), where the normalization is with respect to the characteristic impedance of air. The physical damping of the incoming pressure waves by the dissipation of its kinetic energy is described using the real part of the impedance, i.e., the resistance ($\Re$). It is governed by Equation (1) [7]:

$$\Re = real(\bar{Z}) = real\left({P_3 - P_0}/{P_{3-} - P_{3+}} \right),\tag{1}$$

where P_0 is the pressure wave amplitude measured by a microphone flush mounted on the duct wall at the intersection of duct- 1 and -2, opposite to the perforate, and P_{3-}, P_{3+} are the decomposed pressure wave amplitudes in duct-3, as shown in Figure 1. Determination of P_0 can also be done averaging the total acoustic pressure wave amplitudes in duct-1 and -2, as shown in Ref. [7].

Apart from the resistance, the relation of the incoming and outgoing sound waves with respect to the sample are also studied using the three-port scattering matrix (S-Matrix), as governed by Equation (2) [4]:

$$\begin{bmatrix} P_{1+} \\ P_{2+} \\ P_{3+} \end{bmatrix} = \begin{bmatrix} \rho_1 & \tau_{2\to1} & \tau_{3\to1} \\ \tau_{1\to2} & \rho_2 & \tau_{3\to2} \\ \tau_{1\to3} & \tau_{2\to3} & \rho_3 \end{bmatrix} \begin{bmatrix} P_{1-} \\ P_{2-} \\ P_{3-} \end{bmatrix}, or\ \mathbf{P^+} = \mathbf{SP^-}\ , \tag{2}$$

where $P_{x\pm}$ is the decomposed wave pressure amplitudes in duct x. The subscripts '+' and '-' depict the directions as per Figure 1, ρ and τ describe the reflection and transmission coefficients, respectively, and the subscripts represent the respective ducts.

In Equation (1), directly using P_0 from the measured pressure wave amplitudes makes it susceptible to the presence of anti-nodes present at the microphone position and by extension errors created due to standing wave pattern. To avoid this, resistance can also be determined using S-Matrix coefficients as shown in Ref. [7], using Equation (3).

$$\overline{Z_1} = \frac{(\rho_1+\tau_{1\to2}+1)}{2\tau_{1\to3}} - 1\ , \overline{Z_2} = \frac{(\rho_2+\tau_{2\to1}+1)}{2\tau_{2\to3}} - 1\ , \overline{Z_3} = \frac{1+\rho_3}{1-\rho_3} - \frac{1}{2}\left(\frac{\tau_{3\to1}+\tau_{3\to2}}{1-\rho_3}\right), \tag{3}$$

where $\overline{Z_x}$ is the normalized transfer impedance measured under acoustic excitation from duct- x.

The sample under study is a 25mm by 120mm perforated plate with a porosity (σ) of 2.54%, diameter (d) and thickness (t) of 1.2mm and has square-edged perforations. All the measurements were performed at room temperature and in-duct temperature was monitored using calibrated thermocouples. The error range of the data-acquisition module (NI 9214) is limited to ±0.05°C and an averaging of the acquired temperature for 12s per data point was maintained. Determination of the grazing flow speed was carried out using a pitot static tube of 1.1 mm inner diameter. As determined using the flow profile model in Ref. [7], the bulk velocity was determined by integrating the flow profile across half the cross-section. The range of the bulk velocity in this study was from ≈ 10m/s to ≈ 60 m/s. Data acquisition of the acoustic pressure at a sampling frequency of 25.6kHz was done using flush mounted Brüel and Kjær ¼- inch 4938 type condenser microphones and NI 9234 DAQ modules. The measurement range was 100-2250 Hz to limit the acoustic field in ducts to plane wave mode of propagation. Microphone positioning was carried out following the recommendations of Ref. [8] and wave decomposition was carried out using the wave numbers as proposed in Ref. [9]. The following section compares the effect of operating conditions on the calculated resistance and S-Matrix coefficients, without commenting on the nature of the curves under different flow configurations. The nature of said characteristics under the presence of grazing flow is under study[3, 10-12], and beyond the scope of this paper.

3. EFFECT OF OPERATING CONDITIONS

3.1 Temperature

As the speed of sound is directly proportional to the square-root of temperature, error in the estimation of the in-duct temperature results in incorrect calculation of wavenumber (k), which in turn affects the wave decomposition calculations. Moreover, with an increase in frequency the incorrectly estimated wavelength approaches the sample thickness, leading to an increase in the error rate.

In absence of grazing flow, the deviation in the temperature measured in the main duct (duct-1 and -2) and sidebranch (duct-3), i.e., $T_{Sb} - T_{MD}$, is within the error range of the data acquisition module. However, on addition of flow, a maximum deviation of 0.6°C is observed as shown in Figure 2. This

suggests that individual temperature in both ducts needs to be monitored to avoid errors in wave decomposition and sound field calculations. Figure 3-a and -b show the change in resistance and magnitude of reflection coefficient when the error in the input temperature is ± 0.5°C. As the phase difference created by the temperature difference is only dependent on the frequency, the error in the phase angle of the reflection coefficient remains constant across all flow speeds as shown in Figure 3-a. On the other hand, following Equation (3), error in determining the resistance is also dependent on the magnitude of the S- Matrix coefficients at a particular flow speed. Hence the absolute value of error changes with change in the flow speed, as shown in Figure 3-b.
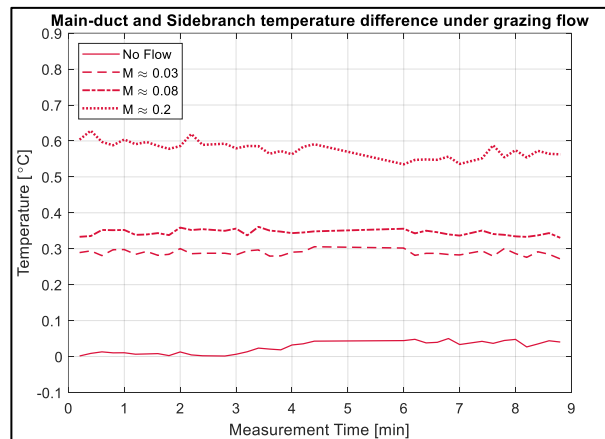

Figure 2 Difference between the main-duct and side branch temperature under the presence of grazing flow in the main duct
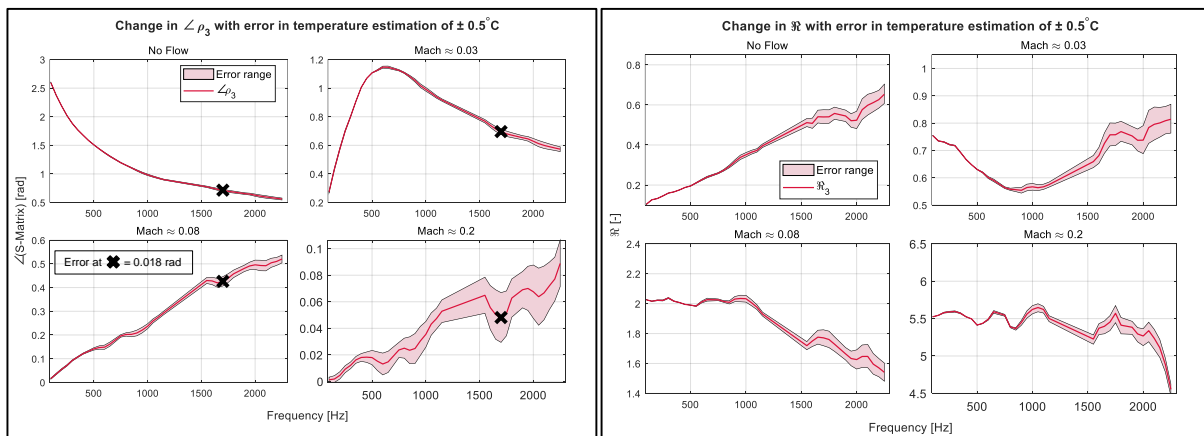

Figure 3 Error estimate of **a)** Phase angle of Reflection Coefficient, and **b)** Normalized Resistance with an error in input temperature of 0.5°C

Table 1 tabulates the maximum error of acoustic characteristics representing the sound field in the side branch, if the entire three-port is calculated only using the temperature measured in the main duct. The phase angle of S-Matrix coefficients $\rho_3, \tau_{3\to1}$, and $\tau_{3\to2}$, as well as the resistance under excitation from the main duct and from the sidebranch directions ($\Re_{MD}, \Re_3$) are considered. As the error observed is proportional to the frequency, the maximum error is observed at the highest frequency considered in the study, i.e., at 2250 Hz.

It can be clearly seen that with an increase in the temperature difference between the ducts, the maximum error of the phase angles increases. However, the error rate of the resistance does not constantly increase. This is because the reference value with respect to which the error is calculated increases significantly. Thus, even while the absolute value of the error increases with an increase in flow speed (and by extension the temperature difference), the change is not reflected in percentages.

Table 1 Error range of acoustic characteristics of the perforate if the sound field is calculated using only the main-duct temperature as input

Grazing flow speed [Mach Number]	Max. Error [%]		Max. Error [rad]		
	$\mathfrak{R}_{MD}$	$\mathfrak{R}_3$	$\angle\rho_3$	$\angle\tau_{3\to1}$	$\angle\tau_{3\to2}$
$0 \ (T_{Sb} - T_{MD} \approx 0.02°C)$	1.2	1.6	0.003	0.002	0.002
$\approx 0.03 \ (T_{Sb} - T_{MD} \approx 0.3°C)$	3	5.1	0.011	0.007	0.007
$\approx 0.08 \ (T_{Sb} - T_{MD} \approx 0.35°C)$	1.4	4.2	0.015	0.009	0.009
$\approx 0.2 \ (T_{Sb} - T_{MD} \approx 0.58°C)$	0.3	2.3	0.017	0.011	0.011

3.2 Flow Speed

The wavenumber of the propagating sound wave depends on the grazing flow Mach number in the main duct as shown in Ref. [9]. Hence errors in the Mach number determination by extension affects the calculated acoustic characteristics.
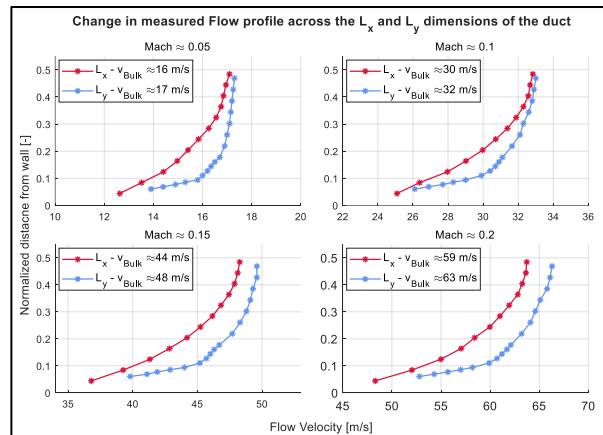

Figure 4 Difference in the flow profile measured across the two cross sections of the main duct

Figure 4 shows the deviation in the flow profile if it is measured across the two cross sections of the duct, where $L_x = 25$mm and $L_y = 120$mm. The normalized distance from the wall (Y-axis) is defined as the ratio of the distance from the wall to the duct dimension ($L_{x,y}$). Flow profile across half the cross-section is measured and as shown, the behaviour of the curve deviates across both the cross sections with an error in the bulk velocity of $\approx 7\%$ across all flow speeds. As in Ref. [13] the flow profile across the L_x dimension is used to calculate the bulk velocity (U_{L_x}). It was found that the

ratio between the bulk velocity and the maximum flow velocity across the cross section, i.e., at the center of the cross section is 0.92, the same as the results of Ref. [13].

A semi-empirical model determined by Kooi and Sarin in Ref. [11] proposes the resistance calculated using skin-friction velocity (u_τ), which is again dependent on the bulk velocity, as shown in Ref. [7]. Since u_τ is directly proportional to U_{bulk} the error in the determination of u_τ is also $\approx 7\%$ if the flow velocity is determined using the flow profile across the L_y dimension.

Table 2 shows the error range across all frequencies in the determined resistance, and the magnitude of the S-Matrix coefficients when the bulk velocity for the post-processing is calculated based on the flow profile across the L_y dimension (U_{L_y}).

A significant increase in the error of $|\rho_{1,2}|$ is seen at high flow speeds due to low reference value (≈ 0.1) of the reflection coefficients at high flow speeds. As the end of the side branch is sealed, the mean flow speed in the side branch (duct- 3) is zero. Thus, as per Equation (1), the resistance is theoretically unaffected by the error in the determination of the flow speed. However, since $\Re_3$ is determined using Equation (3), although comparatively low, an error in the flow speed estimate is reflected in the calculated resistance.

Table 2 Error range of acoustic characteristics of perforate if the sound field is calculated using the bulk velocity across the L_y dimension

Grazing flow speed [Mach Number]	Error range [%]				
	$\Re_{MD}$	$\Re_3$	$|\rho_1|$	$|\rho_2|$	$|\tau_{1 \to 2}|$
$\approx 0.05\ (U_{L_y} - U_{L_x} \approx 1$ m/s)	0 to 8.2	0 to 0.8	0 to 13.5	0 to 13.8	0 to 1.2
$\approx 0.1\ (U_{L_y} - U_{L_x} \approx 2$ m/s)	0 to 3	0 to 0.3	0 to 19.6	0 to 14.7	0 to 1.2
$\approx 0.15\ (U_{L_y} - U_{L_x} \approx 4$ m/s)	0 to 5.7	0 to 0.6	0 to 36.3	0.5 to 73.5	0 to 2.4
$\approx 0.2\ (U_{L_y} - U_{L_x} \approx 4$ m/s)	0 to 6.9	0 to 0.7	0.6 to 65.8	1.7 to 156.3	0 to 2.8

3.3 Microphone Distances

For an empty T-Junction (in absence of a perforate at the cross section), a length correction to be added to the side branch is proposed in Ref. [4, 5], to determine the origin point of the three- port i.e., the physical dimension where the three-port collapses. The addition of this extra length is to compensate for the near field effects observed at the opening of the side branch. A similar approach is used in determining the origin point of the T-Junction with a perforate in Ref. [6], where comparing the phase angle of the transmission coefficients of the perforate in a two-port impedance tube and three-port, the extra length is calculated. The extra length added to the side branch was ≈ 2mm. However, it was later found that the near field effect after placing the perforate is minimal due to the low porosity of the perforate, suggesting that the approach is incorrect. The incorrect results obtained in Ref. [6] without the implementation of the length correction were due to the errors in the calculation of the microphone distances and incorrect temperature estimation in the side branch. The validation of the origin point of the three-port in this study is done by comparing the acoustic characteristics obtained under acoustic excitation from all the three directions, in the absence of grazing flow. It is

found that when the center of the perforate is taken as the origin point of the three-port, the results from all three directions of incidence match each other.

An error in the estimation of microphone distance leads to the incorrect positioning of the origin point of the three-port and affects the sound field calculated. Table 3 shows the error in the calculated acoustic characteristics if the origin point of the three-port is shifted by 1mm away from the center of the perforate along the axis of the side branch.

Since the phase angles of the S-Matrix coefficients are only dependent on frequency, across all flow speeds the maximum error remains constant. As per the definition of S-Matrix in Equation (2), under anechoic termination, ρ_3 is the ratio of P_{3+} and P_{3-}, where as $\tau_{3\to1,2}$ is the ratio of $P_{1,2+}$ and P_{3-}. Since $P_{1,2+}$ are unaffected by the shifting of the three-port origin across the sidebranch axis, but $P_{3\pm}$ are affected, the error in case of ρ_3 is double than that of $\tau_{3\to1,2}$. In case of the resistance, with an increase in the grazing flow speeds, the error changes similar to that in Table 1, as in both cases, incorrect estimation of the wavenumber leads to these errors. To give an insight into the error observed in the resistance values over the frequency range, Table 3 also shows the frequency till which the error rate is less than 10%.

Comparing the ratio of the average error across the entire frequency range for incorrect temperature and incorrect distances, it was found that a shift in the origin by 1mm gives an error equivalent to that of an incorrect temperature of $\approx 1.8°C$.

Table 3 Error range of acoustic characteristics of perforate if the sound field is calculated at 1mm distance away from the three-port origin point

Grazing flow speed [Mach Number]	Max. Error [%]		Frequencies till which error is < 10% [Hz]		Max. Error [rad]		
	$\Re_{MD}$	$\Re_3$	$\Re_{MD}$	$\Re_3$	$\angle\rho_3$	$\angle\tau_{3\to1}$	$\angle\tau_{3\to2}$
0	27.2	28.7	1200	1050			
≈ 0.03	18.2	25.8	1650	1250			
≈ 0.08	6	17.5	-	1750	0.082	0.041	0.041
≈ 0.2	0.3	12.1	-	1750			

4. SUMMARY AND FUTURE WORKS

The effect of experimental errors in determining the operating conditions on the acoustic characteristics of a perforate using a three-port technique is shown in this study. Causes of the individual errors in acquisition of in-duct temperature, grazing flow speed and microphone distances are discussed. Although physically, the effect of a minor change in said conditions does not affect the sound field in three-port significantly, however, usage of these incorrect values in the post-processing and the magnification of the error on the calculated acoustic characteristics, i.e., the transfer impedance and the scattering matrix are portrayed here. Changes in the maximum error on the addition of grazing flow in the three-port is discussed and reasons explaining the behaviour of the error with respect to the flow speeds are given. Future work includes a study of the errors in the acquisition of pressure signals by the microphones, and their effect on the results. Moreover, a Monte Carlo simulation to study the effect of all the erroneous operating conditions simultaneously is also planned.

6. REFERENCES

[1]   Jones, M.G. , Watson, W.R., Howerton, B.M. and Busse-Gerstengarbe, S., *Comparative study of Impedance Eduction Methods, Part 2: NASA Tests and Methodology*, in *19th AIAA/CEAS Aeroacoustics Conference*. 2013.

[2]   Zhou, L., Bodén, H., Lahiri, C., Bake, F., Enghardt. L and Elnady T. , *Comparison of impedance eduction results using different methods and test rigs*, in *20th AIAA/CEAS Aeroacoustics Conference*. 2014: Atlanta, GA.

[3]   Dickey, N.S., Selamet, A. and Ciray, M.S., *An experimental study of the impedance of perforated plates with grazing flow*. Journal of Acoustical Society of America, 2001. **110**: p. 2360-2370.

[4]   Karlsson, M. and Åbom, M., *Aeroacoustics of T-junctions-an experimental investigation.* Journal of Sound and Vibration, 2010. **329**: p. 1793-1808.

[5]   Holmberg, A., Karlsson, M. and Åbom, M., *Aeroacoustics of rectangular T-junctions subject to combined grazing and bias flows - An experimental investigation.* Journal of Sound and Vibration, 2015. **340**: p. 152-166.

[6]   Shah, S., Bodén, H. and Boij, S., *Experimental study on the acoustic properties of perforates under flow using three-port technique*, in *27th International Congress on Sound and Vibration*. 2021: Prague.

[7]   Shah, S.A., Bodén, H., Boij, S. and D'elia, M.E., *Three-port Measurements for Determination of the Effect of Flow on the Acoustic Properties of Perforates*, in *AIAA AVIATION 2021 FORUM*. 2021: Virtual Event.

[8]   Åbom, M. and Bodén, H. , *Error analysis of two-microphone measurements in ducts with flow.* The Journal of the Acoustical Society of America, 1988. **83**.

[9]   Dokumaci, E., *A Note on Transmission of Sound in a Wide Pipe with Mean Flow and Viscothermal Attenuation.* Journal of Sound and Vibration, 1997. **208**: p. 653-655.

[10] Elnady, T., *Modelling and Characterization of Perforates in Lined Ducts and Mufflers*. 2004, KTH, Stockholm.

[11] Kooi, J.W. and Sarin, S.L., *An experimental study of the acoustic impedance of Helmholtz resonator arrays under a turbulent boundary layer*, in *7th AIAA Aeroacoustics Conference*. 1981.

[12] Guess, A.W., *Calculation of Perforated Plate Liner Parameters from Specified Acoustic Resistance and Reactance.* Journal of Sound and Vibration, 1975. **40**: p. 119-137.

[13] Zhou, L. and Bodén, H., *A systematic uncertainty analysis for liner impedance eduction.* Journal of Sound and Vibration, 2015.